

Angle and distance effect on phosphor thermometry

Qiuyang Yin^{1,2,3,4}, Yongkai Quan^{1,2,3,4}, Long Ma⁴, Jianyu Liu^{1,2,3,4}, Jieming Chai^{1,2,3,4}, Jichen Liu^{1,2,3,4}, Lina Zhang^{1,2,3,4}, *

National Key Laboratory of Science and Technology on Aero-Engine Aero-thermodynamics, Research Institute of Aero-engine, Beihang University, Beijing 100191, China
International Innovation Institute, Beihang University, Hangzhou 311115, China
Tianmushan Laboratory, Hangzhou, 311115, China
Research Institute of Aero-engine, Beihang University, Beijing 100191, China

Abstract

Phosphor thermometry is a non-contact technology that holds promise for measuring temperatures of gas turbine. This paper investigated the effects of angle and distance on phosphor thermometry of four distinct samples. The results revealed that different samples responded differently to angles and distances. For YSZ: Dy and YSZ: Sm powders, the maximum effect on the thermometry results were observed 3% and 12.8%, respectively.

Keywords: Aeroengine, Phosphor thermometry, Angle and distance effect.

1. Introduction

With the development of the aeroengine, the turbine inlet temperature increases gradually which is posing significant challenge to the safety of the aeroengines. Accurate temperature measurements of the hot-end components of aircraft engines are essential for the design of effective thermal management systems and ensuring engine safety. However, few temperature measurement techniques can operate in such extreme environments. The thermocouples interfere with the temperature field of the surface being measured. While infrared thermometry results are highly sensitive to changes in emissivity [1]. Phosphor thermometry holds promise for measuring gas turbine temperatures due to its non-contact characteristics and independence of emissivity.

The application of phosphor thermometry technology in aeroengines is to dope rare earth ions into the thermal barrier coating to make it have phosphorescence characteristics. When the thermal barrier coating is excited by a laser, it will radiate phosphorescence, which is temperature dependent. There are two main methods of phosphor thermometry to measure temperature, lifetime decay method and fluorescence intensity ratio (FIR) method [2]. The lifetime decay method relies on monitoring the temperature-dependent lifetime of rare earth ions to determines the temperature. The FIR method estimates temperature by calculating the ratio of emission intensities at two wavelengths, corresponding to thermally coupled energy levels. The population of rare earth ions distributed on thermally coupled levels depends on temperature, which implies that temperature affects the intensity ratio associated with the thermally coupled energy levels. The FIR method is independent of spectrum losses and fluctuations in the excitation intensity [3]. Therefore, the FIR method is widely utilized and is extensively regarded as a promising technique for temperature measurement [4].

Although phosphor thermometry exhibits great potential for precise temperature measurements, the harsh engine environment brings a lot of challenges to the application of phosphorescence thermometry. High operating temperatures, intense background radiation, diverse component geometries, and rapid rotation speeds make it difficult to generalize a universal measurement solution for all engine components [5]. Adhering the phosphor to the surface of interest in high operating temperature environments is vital for the successful implementation of phosphor thermometry. Various commercially available binders have been investigated to ensure great adhesion [6, 7]. Furthermore, blackbody radiation in high temperature environment may drown the signal and lead to

test failures. Cai et al proposed a correction method for thermal radiation errors in high-temperature measurements [8]. However, the influence of angle variations due to turbine blade geometry and distance variations due to rotation on phosphor thermometry are still elusive and requires further exploration.

This paper investigated the impact of angle and distance on phosphor thermometry, focusing specifically on lanthanide ion-doped (Ln = Dy, Sm) yttria-stabilized zirconia (YSZ) and yttrium aluminum garnet (YAG). Four distinct samples, YAG: Dy powder, YSZ: Sm powder, YSZ: Dy powder, and YSZ: Dy coating, were studied. The emission spectra of four samples were obtained when the angle varied from 0° to 85° and when the distance ranged from 100cm to 195cm. The intensity variation with angle and distance at two specific wavelengths that were utilized to assess temperature using the intensity ratio method was analyzed. The intensity ratio for phosphor thermometry under different angles and distances was calculated.

2. Experimental setup

Four distinct samples were examined in this research. Three of them were powder, another one was coating. The powder samples of YSZ: 1% Dy, YAG: 5% Dy, and YSZ: 1% Sm were prepared by coprecipitation method. The coating of YSZ: Dy was synthesized by air plasma spraying based on the powder of YSZ: 1% Dy.

In order to investigate the effects of angle and distance on phosphor thermometry, a rotation platform with a micrometer was employed to control the angle of the samples. Additionally, a 1-meterlong guide rail was utilized to adjust the distance of the samples. The schematic diagram of experimental setup is shown in Figure 1. Each powder sample was compacted in an aluminum oxide container. The coating sample or aluminum oxide container containing the powder sample, was securely fastened in an optics adjustment frame, which was firmly fixed to the rotation platform. The rotation platform was mounted onto the guide rail by slide blocks. The near end of the guide rail was positioned 1m away from the monochromator.

Before the formal experiment, both the angle of the guide rail and the rotation platform were calibrated to ensure that the guide rail was parallel to the laser beam, and the rotation platform was adjusted to 0° coincided with the angle with the maximum phosphorescence intensity. Firstly, the angle of the guide rail was calibrated. A laser safety screen with scales was installed on the slide block, which was mounted on the guide rail. The position of the slide block equipped with the laser safety screen on the guide rail was adjusted. When the position of the laser spot on the laser safety screen remained unchanged at different positions of the slide block, the guide rail was parallel to the laser beam. Secondly, the angle of the rotation platform was calibrated. A coating sample was held in an optics adjustment frame securely attached to the rotation platform, which was mounted onto the guide rail by slide blocks. By varying the angle of the rotation platform, this study identified the specific angle that exhibited maximum phosphorescence intensity.

After the calibration process, spectra were collected at 5-degree intervals to estimate intensity and intensity ratio for angles in the range of 0° and 85°. To determine the distance effect on phosphor thermometry, the position of the rotation platform along the guide rail was varied. Spectral acquisition positions to calculate intensities and intensity ratios were set at distances of 100 cm, 120 cm, 140 cm, 160 cm, 180 cm, and 195 cm from the monochromator.

The sample was excited by a laser and the phosphorescence emitted by the sample was detected by the spectrograph. Excitation was achieved using pulsed Nd: YAG lasers operating at 355 nm. The output energy was 100mJ and the repetition rate was 10 Hz. The laser went through a mirror and a dichroic beam splitter to excite the sample. The dichroic beam splitter was a single edge laser dichroic beam splitter. Its transmission band was 367-1200nm, the transmittance of the transmission band was greater than 90%. Its reflection band was 325-355nm, with reflectivity exceeding 94%. This dichroic beam splitter allowed phosphorescence to pass through while blocking the laser from passing through. Phosphorescence emitted by the samples passed through the dichroic beam splitter, and lens, and finally detected by the spectrograph and the ICCD detector. The ICCD detector was triggered by the lasers. The phosphorescence signal was converted to electronic signal and transmitted to a computer by the ICCD detector.

In order to minimize the random error of the experiment and mitigate the effects of background

noise, both phosphorescence spectra and background noise spectra were collected 20 times at each position. The average of 20 phosphorescence spectra minus the average of 20 background noise spectra was taken as the result of the working condition.

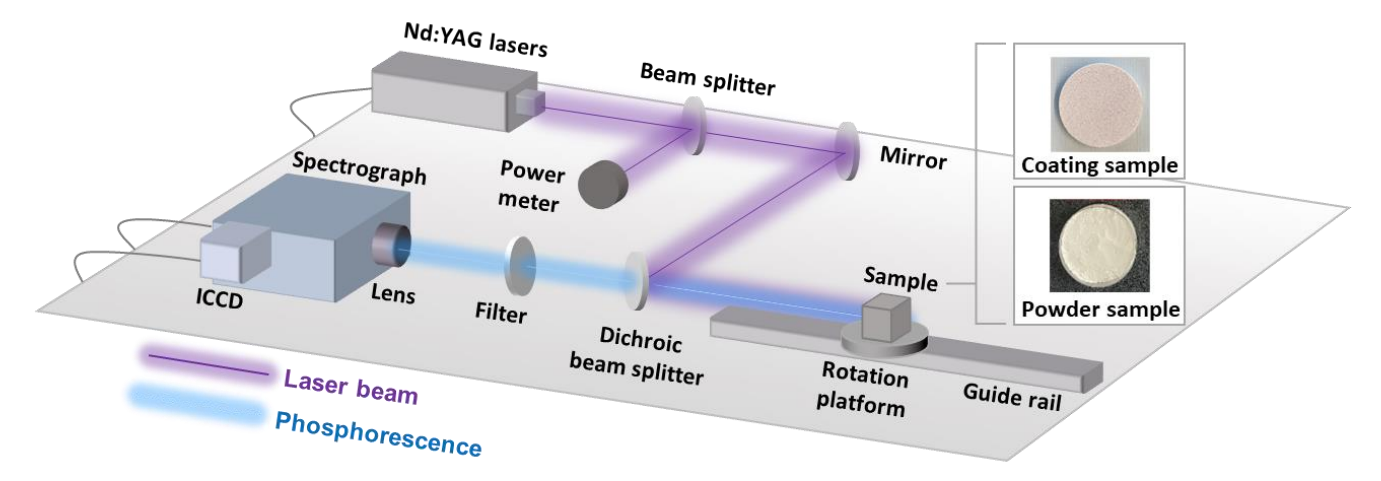


Figure 1 - Schematic of experimental setup

According to the principle of intensity ratio method of phosphor thermometry, the intensity ratio of some wavelength couples radiated by rare earth ions is temperature dependent. The relationship between temperature and the phosphorescence intensity ratio is shown in Eq.(1).

$$FIR = Be^{-\frac{\Delta E}{k_B T}} + C \tag{1}$$

Where FIR is the fluorescence intensity ratio, B is a coefficient determined by fitting, ΔE is the energy level difference between the energy levels corresponding to the two wavelengths used for the ratio of the intensities, k_B is Boltzmann's constant, T is the temperature, and C is the fitting coefficient due to the overlap of the two emission peak bands and the presence of stray light.

Based on the luminescent properties of phosphor powders and error analysis theory, the wavelength couples of the four samples were optimized to obtain the highest temperature measurement accuracy. The optimal working wavelength couple of YSZ: Sm powder was 598nm and 628nm, while the optimal working wavelength couple of the other three samples was 466nm and 488nm.

3. Result and Discussion

3.1 Angle effect

The angle effects of YAG: Dy powder and YSZ: Sm powder are shown in Figure 2. Figure 2 a) and d) illustrate the emission spectra of YAG: Dy powder and YSZ: Sm powder at different angles. The emission wavelength range of YAG: Dy powder was from 440 nm to 610 nm, and there were two main emission bands, located from 440 nm to 510 nm and from 560 nm to 610 nm. The emission wavelength range of YSZ: Sm powder was from 540 nm to 700 nm. The wavelength of the emission spectra did not change with the angle, whereas the intensity of the emission spectra varied with the angle. The intensity of YAG: Dy powder and YSZ: Sm powder both decreased with the increasing angle. The spectra of YSZ: Sm powder was acquired by ICCD with the intensifier in an open state, but the spectra of YAG: Dy powder were obtained without the utilization of the intensifier. Notably, the magnification of the intensifier was 40. Therefore, the intensity of YAG: Dy powder was much stronger than YSZ: Sm powder.

As presented in Figure 2 b) and e), the intensity of YAG: Dy powder and YSZ: Sm powder both decreased with the addition of angle. The effect of angle on the intensity of YAG: Dy powder and YSZ: Sm powder at different wavelengths was consistent. The rate of decrease was more and more fast, which can be explained by Lambert's cosine law [9]. In this study, the incidence angle and the emergence angle were the same according to the experimental setup. When the incidence angle of the laser is θ , the emergence angle is also θ , and the actual receiving radiation will be proportional to the cosine of the incidence angle. The reason for the non-smooth curve may be the uneven surface of the powder.

As illustrated in Figure 2 c) and f), the intensity ratio of YAG: Dy powder barely varied with angle, the maximum deviation from the mean value of intensity ratio was only 0.86%, but the intensity ratio of YSZ: Sm powder increased and then decreased as the angle increased, the maximum deviation from the mean value was 12.8%. The possible reason for this phenomenon is the low signal intensity of YSZ: Sm powder. When the angle increased, the signal of YSZ: Sm weakened and the signal-tonoise ratio decreased, resulting in the deviation of the intensity ratio. If the signal above 50 degrees is removed, the maximum deviation from the average will be reduced to less than 4%.

The angle effects of YSZ: Dy powder and YSZ: Dy coating are presented in Figure 3. Figure 3 a) and d) illustrate the emission spectra of YSZ: Dy powder and YSZ: Dy coating at different angles. The emission wavelength range of YSZ: Dy powder and the YSZ: Dy coating were both from 440 nm to 610 nm, and there were two main emission bands, located from 440 nm to 510 nm and from 560 nm to 610 nm. The wavelength range was consistent with YAG: Dy powder because the same rare earth ion, but the shapes of spectra were different due to the distinct host.

The effect of angle on the intensity of YAG: Dy powder and YSZ: Sm powder at different wavelengths was consistent. The variation of intensity of YSZ: Dy powder and YSZ: Dy coating with angle was in agreement with that of YAG: Dy powder and YSZ: Sm powder, suggesting that Lambert's cosine law applied to the change of intensity with angle. The difference in decay rate of different samples may be caused by the unevenness of the powder sample plat.

The intensity-angle curve of the coating was smoother than that of the powder because the coating surface was relatively flat. The maximum deviations of intensity ratio from the mean value were 3% and 0.56% for powder and coating, respectively.

3.2 Distance effect

The distance effects of YAG: Dy powder and YSZ: Sm powder are demonstrated in Figure 4. Figure 4 a) and d) display the spectra of YAG: Dy powder and YSZ: Sm powder at different distances. The intensity of YAG: Dy powder and YSZ: Sm both decreased with the increasing distance. The wavelength of the emission spectra remained constant as the distance changed, but the intensity of the emission spectra fluctuated according to the distance.

As shown in Figure 4 b) and e), the intensity of YAG: Dy powder and YSZ: Sm powder initially dropped quickly then gradually decreased as the distance rose, because the phosphorescence intensity changed with the distance following the inverse square law [10]. The inverse square law indicates that the phosphorescence intensity is inversely proportional to the square of the distance. In particular, at large distances from the source, the radiation intensity is distributed over surfaces and therefore the intensity per unit area decreases as the distance from the surface to the source increases. The phosphorescence intensity progressively and more slowly diminished with increasing distance. The effect of distance on the intensity of YAG: Dy powder and YSZ: Sm powder at different wavelengths was consistent.

As illustrated in Figure 4 c) and f), the intensity ratio of YAG: Dy powder barely varied with distance, the maximum deviation from the mean value was only 0.3%, but the intensity ratio of YSZ: Sm powder increased and then fell as the distance increased, the maximum deviation from the mean value was 4.8%. The possible reason for this phenomenon is the low signal intensity of YSZ: Sm. When the distance increased, the signal of YSZ: Sm weakened and the signal-to-noise ratio dropped, resulting in the divergence of the intensity ratio from average value. If the signal above 160 cm is removed, the maximum deviation from the average will be reduced to less than 1.35%.

The distance effects of YSZ: Dy powder and YSZ: Dy coating are presented in Figure 5. Figure 5 a) and d) display the spectra of YSZ: Dy powder and YSZ: Dy coating at different distances. The wavelength of the emission spectra did not change with the change of angle, but the intensity of the emission spectra varied with the change of angle. The intensity of YSZ: Dy powder and YSZ: Dy coating decreased with increasing distance. The variation of intensity of YSZ: Dy powder and YSZ: Dy coating with distance was consistent with that of YAG: Dy powder and YSZ: Sm powder, indicating that the inverse square law applied to the intensity variations of all samples. The maximum deviations of intensity ratio from the average value were 0.84% and 0.22% for powder and coating, respectively.

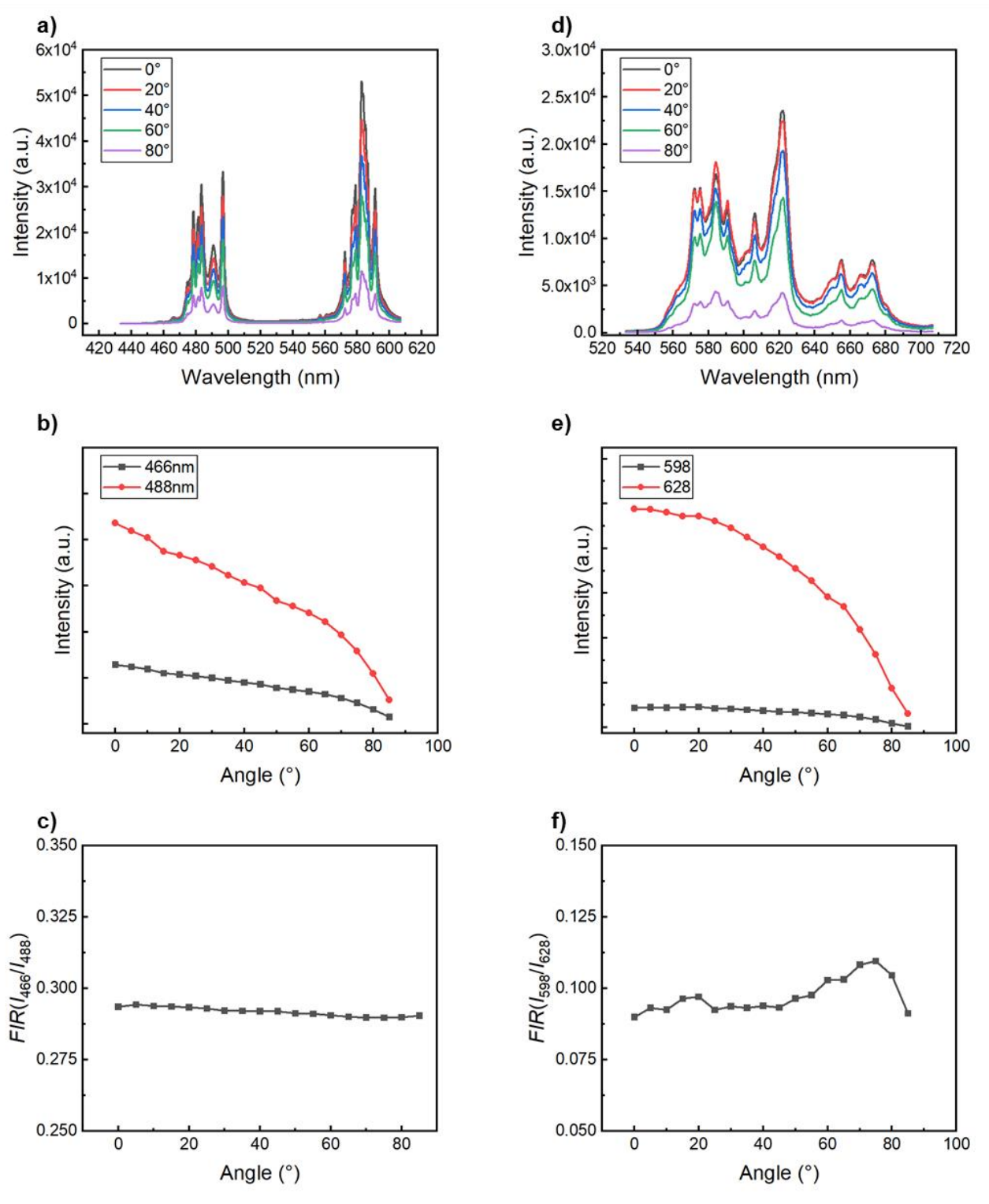


Figure 2 - The angle effects of YAG: Dy powder and YSZ: Sm powder: a) Spectra of YAG: Dy in different angles, b) Variation of intensity of YAG: Dy with angle for wavelengths used for intensity ratio, c) Variation of intensity ratio of YAG: Dy with angle, d) Spectra of YSZ: Sm in different angles, e) Variation of intensity of YSZ: Sm with angle for wavelengths used for intensity ratio, f) Variation of intensity ratio of YSZ: Sm with angle.

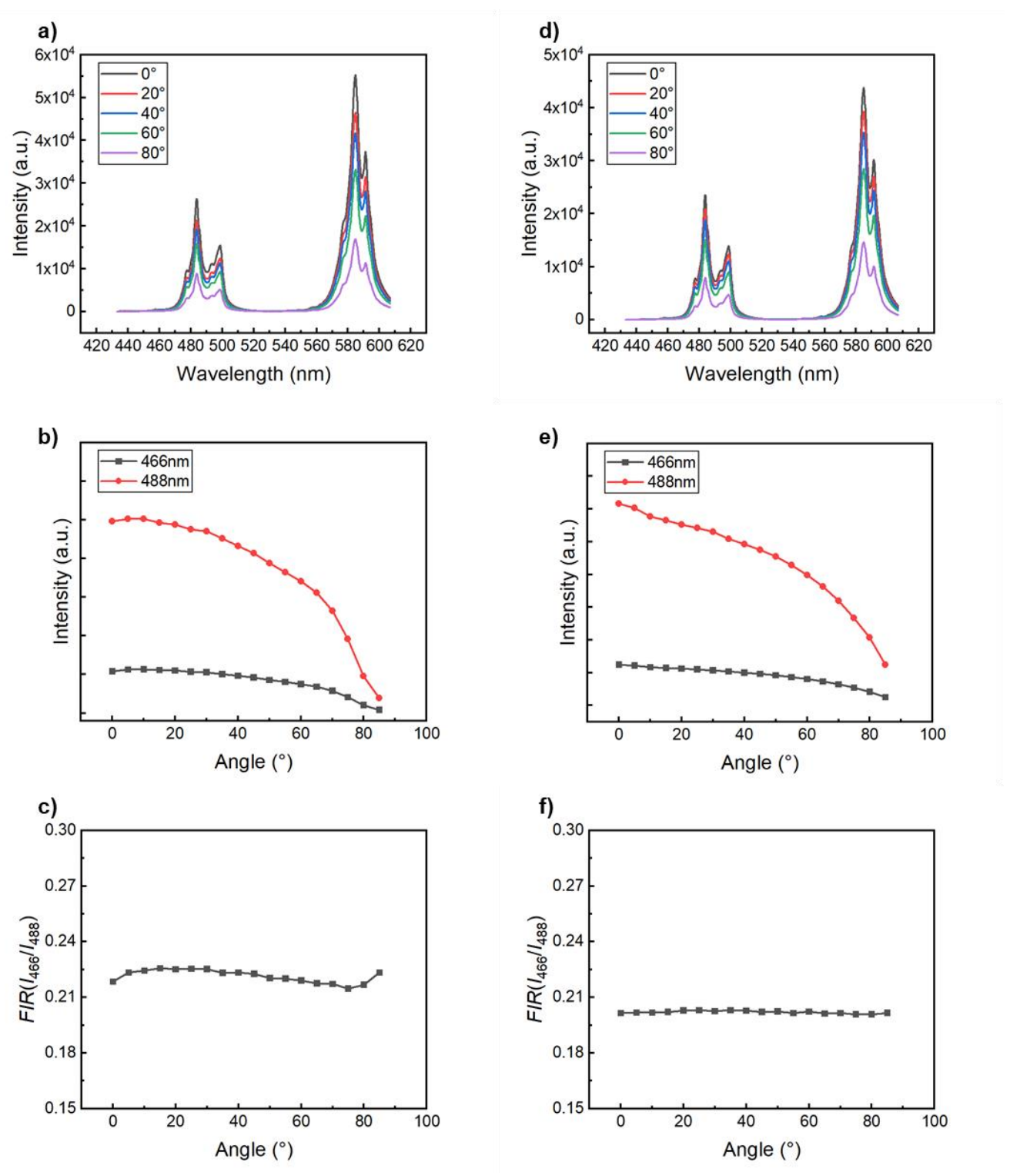


Figure 3 - The angle effects of YSZ: Dy powder and YSZ: Dy coating: a) Spectra of YSZ: Dy powder in different angles, b) Variation of intensity of YSZ: Dy powder with angle for wavelengths used for intensity ratio, c) Variation of intensity ratio of YSZ: Dy powder with angle, d) Spectra of YSZ: Dy coating in different angles, e) Variation of intensity of YSZ: Dy coating with angle for wavelengths used for intensity ratio, f) Variation of intensity ratio of YSZ: Dy coating with angle.

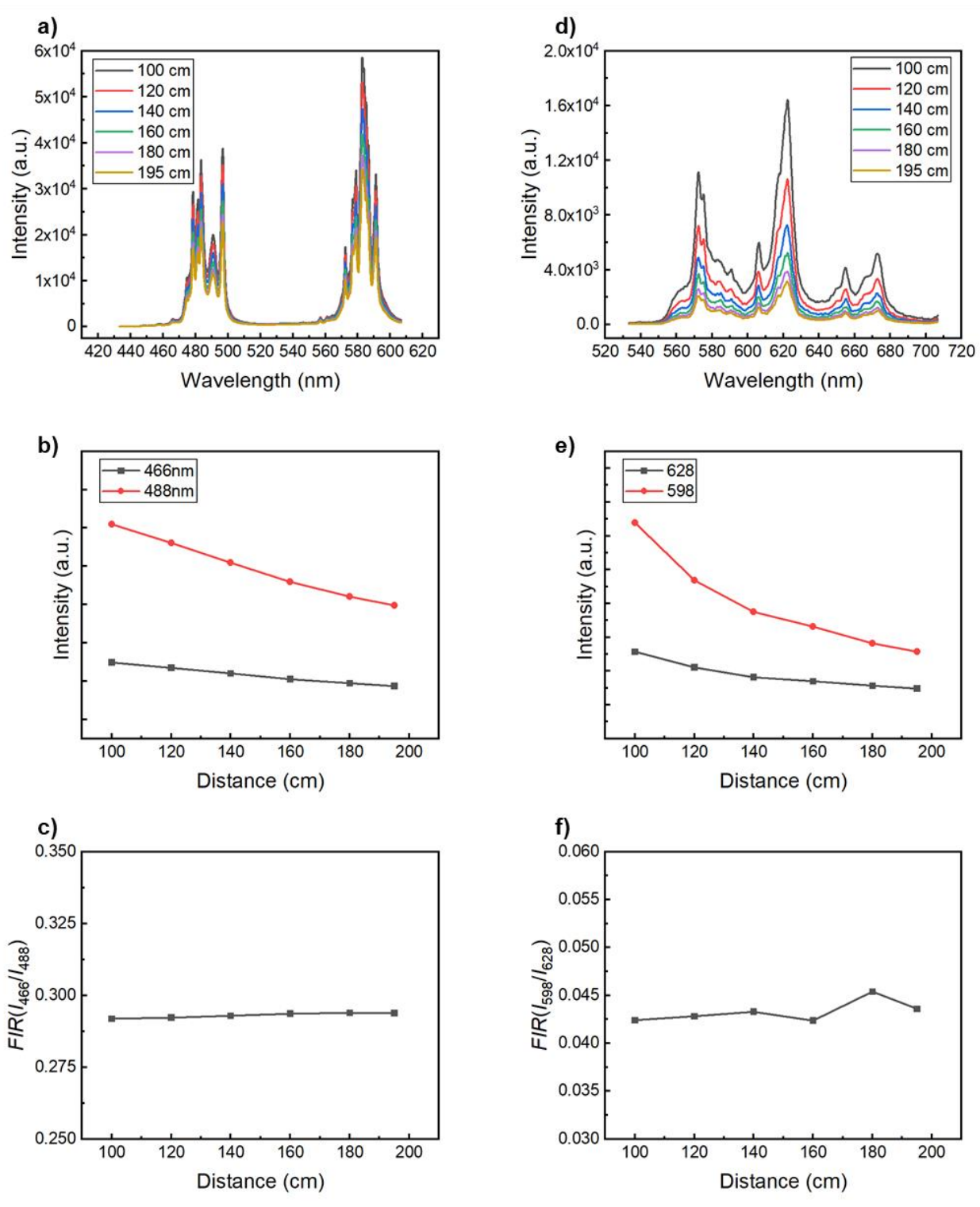


Figure 4 - The distance effects of YAG: Dy powder and YSZ: Sm powder: a) Spectra of YAG: Dy in different distances, b) Variation of intensity of YAG: Dy with distance for wavelengths used for intensity ratio, c) Variation of intensity ratio of YAG: Dy with distance, d) Spectra of YSZ: Sm in different distances, e) Variation of intensity of YSZ: Sm with distance for wavelengths used for intensity ratio, f) Variation of intensity ratio of YSZ: Sm with distance.

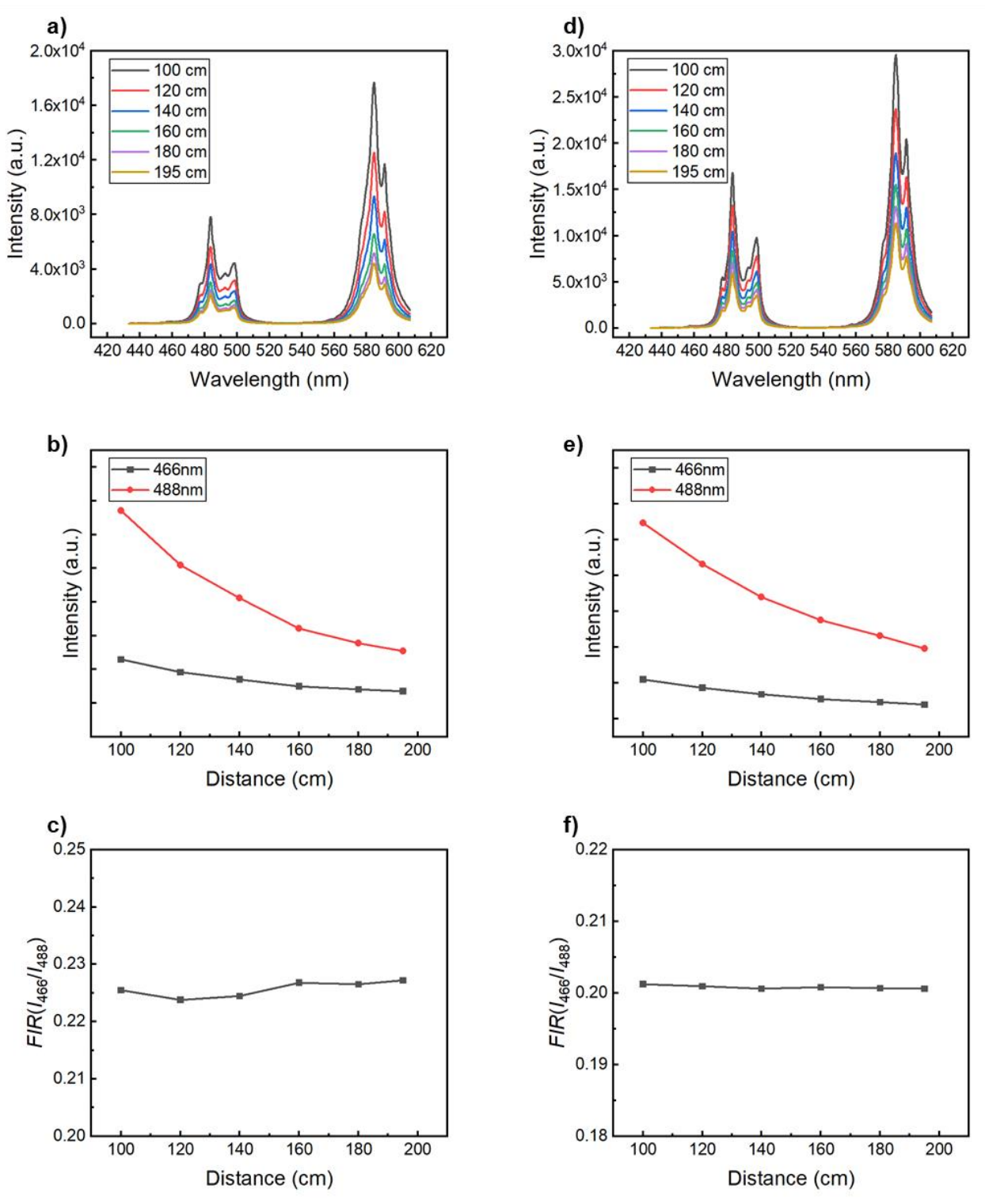


Figure 5 - The distance effects of YSZ: Dy powder and YSZ: Dy coating: a) Spectra of YSZ: Dy powder in different distance s, b) Variation of intensity of YSZ: Dy powder with distance for wavelengths used for intensity ratio, c) Variation of intensity ratio of YSZ: Dy powder with distance, d) Spectra of YSZ: Dy coating in different distance s, e) Variation of intensity of YSZ: Dy coating with distance for wavelengths used for intensity ratio, f) Variation of intensity ratio of YSZ: Dy coating with distance.

4. Conclusion

This paper explored the effects of angle and distance on phosphor thermometry. The emission spectra of four distinct samples, YAG: Dy powder, YSZ: Sm powder, YSZ: Dy powder, and YSZ: Dy coating, were investigated. The variation of intensity with angle and distance of two specific wavelengths used for temperature measurement was analyzed. The intensity ratio for phosphor thermometry under different angles and distances was evaluated. The findings could be summarized as follows.

Angle and distance effect on phosphor thermometry

- 1. Phosphorescent intensity displayed a decreasing trend with both increasing angle and distance. the rate of decrease increased progressively with an increase in angle but decreased gradually with distance.
- 2. Different samples responded differently to angles and distances. The effects of variations in angle and distance on the intensity ratio used for temperature measurement were both less than 1% for YAG: Dy powder and YSZ: Dy coatings, meaning that the intensity ratio utilized for temperature measurement was essentially unaffected.
- 3. The angle significantly affected the intensity ratio used for phosphor thermometry for YSZ: Dy powder and YSZ: Sm powder, which was 3% and 12.8%, respectively. The effect of distance on the intensity ratios of YSZ: Dy powder and YSZ: Sm powder was 0.84% and 4.8%, respectively. If the angle is reduced to 50° or the distance is controlled to 140cm, the error in the intensity ratio of YSZ: Sm powder will be significantly reduced to 4% and 1.35%, respectively.

5. Contact Author Email Address

Qiuyang Yin: yinqiuyang@buaa.edu.cn Tel: +86 15652586809 Or Lina Zhang: zhangln@buaa.edu.cn Tel: +86 13241855836

6. Copyright Statement

The authors confirm that they, and/or their company or organization, hold copyright on all of the original material included in this paper. The authors also confirm that they have obtained permission, from the copyright holder of any third party material included in this paper, to publish it as part of their paper. The authors confirm that they give permission, or have obtained permission from the copyright holder of this paper, for the publication and distribution of this paper as part of the ICAS proceedings or as individual off-prints from the proceedings.

References

- [1] A. H. Khalid and K. Kontis, "Thermographic phosphors for high temperature measurements: Principles, current state of the art and recent applications," (in English), *Sensors*, Review vol. 8, no. 9, pp. 5673-5744, Sep 2008.
- [2] J. S. Zhong *et al.*, "A review on nanostructured glass ceramics for promising application in optical thermometry," (in English), *Journal of Alloys and Compounds*, Review vol. 763, pp. 34-48, Sep 2018.
- [3] L. Li, C. F. Guo, S. Jiang, D. K. Agrawal, and T. Li, "Green up-conversion luminescence of Yb3+-Er3+ co-doped CaLa2ZnO5 for optically temperature sensing," (in English), *Rsc Advances*, Article vol. 4, no. 13, pp. 6391-6396, 2014.
- [4] M. D. Dramicanin, "Trends in luminescence thermometry," *JOURNAL OF APPLIED PHYSICS*, Article vol. 128, no. 4, 2020 JUL 28 2020.
- [5] A. H. Khalid, K. Kontis, and H. Z. Behtash, "Phosphor thermometry in gas turbines: consideration factors," *PROCEEDINGS OF THE INSTITUTION OF MECHANICAL ENGINEERS PART G-JOURNAL OF AEROSPACE ENGINEERING,* Article vol. 224, no. G7, pp. 745-755, 2010 2010.
- [6] S. W. Allison et al., "High temperature surface measurements using lifetime imaging of thermographic phosphors: Bonding tests," presented at the ICIASF'01: 19TH INTERNATIONAL CONGRESS ON INSTRUMENTATION IN AEROSPACE SIMULATION FACILITIES, RECORD, 2001, 2001. Proceedings Paper.
- [7] S. W. Allison *et al.*, "ADVANCES IN HIGH TEMPERATURE PHOSPHOR THERMOMETRY FOR AEROSPACE APPLICATIONS," pp. 1-6, 2003.
- [8] T. Cai, D. Peng, Y. Z. Liu, and X. F. Zhao, "A correction method of thermal radiation errors for high-temperature measurement using thermographic phosphors," *JOURNAL OF VISUALIZATION*, Article vol. 19, no. 3, pp. 383-392, 2016 AUG 2016.
- [9] J. Folkesson, H. Chang, and N. Bore, "Lambert's Cosine Law and Sidescan Sonar Modeling," presented at the IEEE/OES Autonomous Underwater Vehicles Symposium (AUV), ELECTR NETWORK, SEP 30-OCT 02, 2020, 2020.
- [10] C. E. Gutiérrez and A. Sabra, "The reflector problem and the inverse square law," *Nonlinear Analysis: Theory, Methods & Applications*, vol. 96, pp. 109-133, 2014.